

PNIPAm-PEO-PPO-PEO-PNIPAm Pentablock Terpolymer: Synthesis and Chain Behavior in Aqueous Solution

Aixiong Mei,[†] Xiaolei Guo,[†] Yanwei Ding,[‡] Xinghong Zhang,[†] Juntong Xu,[†] Zhiqiang Fan,[†] and Binyang Du^{*†}

[†]MOE Key Laboratory of Macromolecular Synthesis and Functionalization, Department of Polymer Science & Engineering, Zhejiang University, Hangzhou 310027, China, and [‡]Hefei National Laboratory for Physical Sciences at Microscale, University of Science and Technology of China, Hefei, Anhui 230026, China

Received May 16, 2010; Revised Manuscript Received July 22, 2010

ABSTRACT: The double thermosensitive and narrow dispersed PNIPAm₁₁₀-PEO₁₀₀-PPO₆₅-PEO₁₀₀-PNIPAm₁₁₀ pentablock terpolymer was synthesized by the typical atomic transfer radical polymerization (ATRP) method with *N*-isopropylacrylamide (NIPAm) as the monomer and modified poly(ethylene oxide)₁₀₀-poly(propylene oxide)₆₅-poly(ethylene oxide)₁₀₀ (PEO₁₀₀-PPO₆₅-PEO₁₀₀) block copolymer as the macroinitiator. Micro-differential scanning calorimetry (micro-DSC) data showed that the pentablock terpolymer exhibited two low critical solution temperatures (LCSTs) at 31 and 34 °C in the aqueous solution, which can be attributed to the thermal phase transition of the PPO block and PNIPAm block, respectively. The chain conformation of the pentablock terpolymer in aqueous solution was then studied in detail by using a combination of static and dynamic laser light scattering (SLS-DLS). The SLS-DLS results indicated that the loose “associates” and single coil chains coexisted in the aqueous solution at the low temperature, where the PEO, PPO, and PNIPAm blocks were soluble in water. These phenomena were inconsistent with those observed in other PEO-containing block copolymer systems. At the high temperature above the LCSTs of PPO and PNIPAm blocks (38–60 °C), the pentablock terpolymer chains formed large and stable core–shell micelles with collapsed PPO and PNIPAm cores and swollen PEO shells. The TEM and cryo-TEM experiments provided visual images, which confirmed the formation of loose “associates” at 21 °C and large stable micelles at 38 °C. Increase of concentration hindered the formation of “associate” at low temperature, but the micelles formed at high temperature were almost independent of the solution concentration investigated.

Introduction

The chain conformation and solution property of block copolymers in good and selective solvents are long-standing hot topics in the field of polymer physics.^{1–14} Depending on the chain conformation, solutions of block copolymers might have important technological applications, e.g., micelles for drug-controlled release, compatibilizers, or emulsifiers, etc.^{15–17} The chain conformation and solution property of block copolymer are also important for their adsorption behavior on solid surface, which is relevant not only to many technological applications but also to many biological processes. Numerous efforts, including experimental, theoretical, and simulation studies, have been carried out to investigate and understand the chain conformation and solution property of block copolymers.^{18–24} During the past few decades, most of investigations mainly focused on diblock and triblock copolymers because of their relatively simple chain structures.^{25–31}

With the development of new synthetic methods, it is nowadays possible to design and synthesize multiblock copolymers with more complicated chain structures.^{18–21,32–37} Scientific interest and attention are hence also slowly shifted to the chain conformation and solution property of multiblock copolymers, which are thought to be more complex and challenging.^{18–21,38} For pseudo-multiblock copolymer poly(*N*-isopropylacrylamide-*s*-styrene) chains with evenly spaced hydrophobic styrene segments, Zhang et al. observed that these copolymer chains formed single-flower-like core–shell nanoparticles in aqueous solution at temperature ~30.6 °C.³⁹ Flower-like unimolecular and multimolecular micelles

were observed in the aqueous solution of double hydrophilic multiblock copolymers of poly(*N,N*-dimethylacrylamide) and poly(*N*-isopropylacrylamide) (PDMAM_{*p*}-PNIPAm_{*q*})_{*m*} when heating the solution temperature above the LCST of PNIPAm.²¹ Simulation and theoretical studies were also carried out to investigate the micelle behavior of multiblock copolymers in selective solvents and the adsorption of multiblock copolymers on solid surfaces with chemical patterns.^{22–24,40–42} However, the synthesis of multiblock copolymers with the block number > 5 is still less controllable.^{34–36} Especially, it is still difficult to synthesize multiblock copolymers with a narrow molecular weight distribution (< 1.5), which is critical for the study of chain conformation in solution and the adsorption exothermal and kinetic of multiblock copolymer chains on solid surface.

The pentablock copolymers with block number of 5 may be the simplest model and good starting point for the investigation of multiblock copolymers. It is much more easier to synthesize narrow dispersed pentablock by multistep- or one-step-controlled radical copolymerization, like atomic transfer radical polymerization (ATRP) and reversible addition–fragmentation transfer (RAFT) polymerization.^{20,32,43–51} Mallapragada and coauthors carried out pioneer and systematic investigations on the solution properties of a series of pentablock terpolymers,^{20,43,44} which were synthesized by one-step ATRP with modified poly(ethylene oxide)₁₀₀-poly(propylene oxide)₆₅-poly(ethylene oxide)₁₀₀ (PEO₁₀₀-PPO₆₅-PEO₁₀₀) macroinitiator and amine methacrylate as second monomer, including 2-(diethylamino)ethyl methacrylate (DEAEM), 2-(dimethylamino)ethyl methacrylate (DMAEM), 2-(diisopropylamino)ethyl methacrylate (DiPAEM), and (*tert*-butylamino)-ethyl methacrylate (tBAEM). Note that PEO₁₀₀-PPO₆₅-PEO₁₀₀

*Corresponding author. E-mail: duby@zju.edu.cn.

block copolymer is also named as Pluronic F127. They found that these pentablock terpolymers formed temperature and pH-responsive micelles in dilute aqueous solutions and a pH-responsive, thermoreversible gel phase in concentrated aqueous solutions. By employing static and dynamic light scattering, the formation of flower-like micelles was observed for a pentablock copolymer of $D_{20}\text{-}b\text{-}M_{10}\text{-}b\text{-}D_{20}\text{-}b\text{-}M_{10}\text{-}b\text{-}D_{20}$ in aqueous solution.³² Here, D and M stand for 2-(dimethylamino)ethyl methacrylate and methyl methacrylate, respectively. The number of blocks and chain architectures are thought to have significant effects on the chain conformation of the multiblock copolymer in solution.^{32,52}

In the present work, a double thermosensitive pentablock terpolymer PNIPAm₁₁₀-F127-PNIPAm₁₁₀ was synthesized by the typical ATRP method with NIPAm as the monomer and modified F127 as the macroinitiator. It was well-known that Pluronic F127 and PNIPAm exhibit reversible thermosensitive characteristics in their aqueous solutions, respectively. Because of the different low critical solution temperature of Pluronic F127 and PNIPAm, the combination of Pluronic F127 and PNIPAm rendered the PNIPAm₁₁₀-F127-PNIPAm₁₁₀ pentablock terpolymer-rich chain conformations in aqueous solution depending on the environmental temperature. On the other hand, such pentablock terpolymer was also thought to be meaningful for the construction of thermoresponsive surface adsorption layer with certain nanostructure on solid surface via varying the chain conformation in solution. In order to understand the adsorption behavior on solid substrates and achieve the thermoresponsive surface layer, it is also necessary and important to investigate the solution behavior of the pentablock terpolymer. The chain conformation and solution property of the PNIPAm₁₁₀-F127-PNIPAm₁₁₀ pentablock terpolymer in aqueous solution were thus studied and reported here in detail by using a combination of static and dynamic laser light scattering (SLS-DLS) as well as microdifferential scanning calorimetry (micro-DSC). Transmission electron microscopy (TEM) was also employed as supplementary technique to provide visual images of the chain conformation of the pentablock terpolymer at different temperatures.

Experimental Section

Chemical and Materials. Pluronic F127 with number-averaged molecular weight M_n of 1.26×10^4 was a gift from BASF Co. 2-Bromoisobutryl bromide and N,N,N,N',N'' -pentamethyldiethylenetriamine (PMDETA) were purchased from Acros Organics and used as received. Triethylamine (Shanghai Chemical Reagent) was dried by refluxing in the presence of calcium hydride and distilled prior to use. Tetrahydrofuran and 1,4-dioxane (Shanghai Chemical Reagent) were dried by refluxing in the presence of sodium flakes and distilled prior to use. CuBr (Shanghai Chemical Reagent) was washed with deionized water, acetic acid, ethanol, and ether in turn and then dried in vacuum and stored under nitrogen atmosphere before use. *N*-Isopropylacrylamide (NIPAm: 99%, Acros Organics) was recrystallized three times from toluene/hexane (1:1, v:v) prior to use.

Synthesis of Pluronic F127 ATRP Macroinitiator. The Pluronic F127 ATRP macroinitiator was synthesized according to a reported method.⁴³ Typically, Pluronic F127 (13.86 g, 1.1 mmol) and THF (50 mL) were added into a dried three-neck flask. After the Pluronic F127 was completely dissolved, triethylamine (0.46 mL, 3.3 mmol) was added under nitrogen atmospheres. The reaction flask was then put into an ice-salt bath at 0 °C, and 2-bromoisobutryl bromide (0.82 mL, 6.6 mmol) was injected. The ice-salt bath was then taken away, and the mixture solution was stirred at room temperature for 24 h. Magnesium sulfate was added into the final mixture under stirring in order to get rid of the trace water. The final solution was centrifuged to remove the precipitated hydrobromide salt and aquo magnesium sulfate. The supernatant was collected and concentrated with a rotary evaporator. Finally, the Pluronic F127 macroinitiator

was precipitated into *n*-hexane at -72 °C, filtered, and dried under vacuum. The conversion of Pluronic F127 to the difunctional 2-bromopropionate Pluronic F127 ATRP macroinitiator was ca. 71.66%.

Synthesis of Pentablock Terpolymer PNIPAm-F127-PNIPAm. A standard ATRP procedure was applied to synthesize the PNIPAm-F127-PNIPAm pentablock terpolymer. Difunctional 2-bromopropionate Pluronic F127 macroinitiator (0.5027 g, 0.039 mmol), NIPAm (4.0021 g, 0.035 mol), 1,4-dioxane (4 mL), and CuBr/CuBr₂ (12.3 mg/2.1 mg, 0.085 mmol/0.0094 mmol) were introduced into a reaction tube. The mixture was degassed with three freezing-evacuation-thawing cycles, and PMDETA (60 μ L) was then injected. The reaction tube was degassed with freezing-evacuation-thawing cycles again, sealed, and put in an oil bath with preset temperature of 80 °C for polymerization. After 24 h, polymerization was terminated by exposure to air. The blue solution was passed through a short aluminum oxide column to remove the catalyst complex. The obtained colorless solution was transferred to dialysis tubes (M_w cutoff = 14 000) and dialyzed against distilled water for 3 days at room temperature to get rid of unreacted chemical reagent. After dialysis, the sample was concentrated with a rotary evaporator and dried under vacuum. In the final purification step, the dried samples were dissolved in THF and precipitated with diethyl ether. The precipitated product was dried under vacuum to give the final purified PNIPAm-F127-PNIPAm pentablock terpolymer.

Instrumentation and Characterization. The molecular weight distribution of pentablock terpolymer was determined by a gel permeation chromatograph (GPC, PL-GPC 220, Polymer Laboratories Ltd.) with tetrahydrofuran as the eluent and monodisperse polystyrene as the calibration standard. Number-average molecular weights, M_n , were calculated from ¹H NMR of the copolymer, which was performed by a 300 MHz Varian Mercury Plus NMR instrument with CDCl₃ as solvent and tetramethylsilane (TMS) as the internal standard.

Microdifferential scanning calorimetry (micro-DSC) measurements were performed by a VP DSC (MicroCal) in Hefei National Laboratory for Physical Sciences at Microscale, University of Science and Technology of China. The pentablock terpolymer was dissolved in deionized water to give a concentration of 0.5 mg/mL. The heating rate was 1.0 °C/min.

The static and dynamic light scattering (SLS-DLS) of the aqueous solutions of the PNIPAm-F127-PNIPAm pentablock terpolymer were carried out by a commercial spectrometer ALV/DLS/SLS-5022 in Hefei National Laboratory for Physical Sciences at Microscale, University of Science and Technology of China. All of the solutions were filtered through 0.45 μ m Millipore PVDF filters into the dust-free light scattering cells before measurements. During the experiment, the sample vial was placed in a brass holder with a precise temperature control. Measurements were carried out after the samples reached equilibrium. The range of scattering angle θ used for SLS was from 30° to 150° with a step of 5°. The apparent weight-average molecular weight ($M_{w,app}$) and the Z-average root-mean-square radius (R_g) of the objects in solution can be determined from the angular dependence of the excess scattering intensity, known as Rayleigh ratio $R_{vv}(q)$, given as

$$\frac{KC}{R_{vv}(q)} \approx \frac{1}{M_{w,app}} \left(1 + \frac{1}{3} R_g^2 q^2 \right) + 2A_2C \quad (1)$$

where $K = 4\pi n^2 (dn/dc)^2 / (N_A \lambda^4)$ and $q = (4\pi n/\lambda) \sin(\theta/2)$, with dn/dc , N_A , λ , n , and θ being the specific refractive index increment of the solution, the Avogadro number, the wavelength of the laser light in vacuum (here $\lambda = 632$ nm), the refractive index of solvent, and the scattering angle, respectively. The dn/dc value of the sample was determined to be $dn/dc = 0.154$ mL/g by using a differential refractometer developed in Prof. Chi Wu's group.⁵³ C was the concentration of the sample solution. In the present measurement, the last term of eq 1, A_2C ,

can be neglected because the sample concentration used was rather dilute and the extrapolation of $C \rightarrow 0$ was not necessary. The average hydrodynamic radius ($\langle R_h \rangle$) and the distribution of ($\langle R_h \rangle$) from the DLS were calculated by using cumulants analysis and the CONTIN routines.

The cloud point of the aqueous solution of PNIPAm-F127-PNIPAm pentablock terpolymer was determined by a Cary 100 Bio UV-vis spectrophotometer with temperature control. The optical transmittance of the aqueous solution was recorded in the range of wavelength from 800 to 400 nm with a step of 1 nm. The aqueous solution was allowed to be equilibrium for 15 min at each measuring temperature. The optical transmittance of the aqueous solution at 400 nm was selected to plot as the function of measuring temperature. The cloud point was determined as the temperature at which the optical transmittance presented the first strong decrease. Two aqueous solutions with concentrations of 0.3 and 0.5 mg/mL were measured.

Transmission electron microscopy (TEM) measurements were carried out by a JEOL JEM-1200 electron microscope operated at an acceleration voltage of 60 kV. TEM samples were prepared as following: the aqueous solutions of the pentablock terpolymer (0.5 mg/mL), phosphotungstic acid (PTA), and Formvar-coated copper grids were placed in an oven with preset temperature, i.e., 21 and 38 °C, respectively, for a half-hour to reach temperature equilibrium. A droplet of sample solution was then dripped onto the copper grids, which were allowed to dry for another half-hour in the oven. Afterward, the samples were stained with PTA. The stained TEM samples were again allowed to dry in the oven before observation.

The morphologies of the "associates" and micelles of the pentablock terpolymer in aqueous solution were also observed with cryogenic transmission electron microscopy (cryo-TEM). The cryo-TEM measurements were carried out in the BioEM lab, State Key Lab of Biocontrol, School of life Sciences, Sun Yat-Sen University, Guangzhou, 510275. For cryo-TEM, the aqueous solution of pentablock terpolymer (0.5 mg/mL) was first equilibrium at 21 and 38 °C for a half-hour, respectively. Afterward, 4 μ L of sample was applied to a holey carbon film grid (R1.2/1.3 Quantifoil Micro Tools GmbH, Jena, Germany) and was absorbed by filter paper. After absorbing, the grid was immediately plunged into precooled liquid ethane for flash frozen. The cryo-grid was held in a Gatan 626 Cryo-Holder (Gatan) and transferred into TEM (JEOL JEM-2010 with 200 kV LaB₆ filament) at -172 °C. The sample was then observed under minimal dose condition at -172 °C.

Results and Discussion

Synthesis of Pentablock Terpolymer PNIPAm-F127-PNIPAm. The PNIPAm-F127-PNIPAm pentablock terpolymer was synthesized by using the conventional ATRP method. The hydroxyl end groups of F127 were first modified with 2-bromoisobutyl bromide to give the difunctional 2-bromopropionate Pluronic F127 macroinitiator. The ¹H NMR spectrum confirmed the successful preparation of F127 ATRP macroinitiator, as shown in Figure 1. The typical ATRP procedure was then applied to synthesize the pentablock terpolymer with NIPAm as the monomer and modified F127 as the macroinitiator. Figure 2 shows the ¹H NMR spectrum of the purified PNIPAm-F127-PNIPAm pentablock terpolymer. Each proton of the pentablock terpolymer can be identified from its ¹H NMR spectrum. The block length of PNIPAm was determined from the ratio of the integrated intensities of the peaks A and F, which were attributed to PPO blocks and PNIPAm blocks, respectively. Based on the length of each block, the pentablock terpolymer was then named as PNIPAm₁₁₀-F127-PNIPAm₁₁₀. The number-average molecular weight M_n of the pentablock terpolymer was also calculated from the ¹H NMR spectrum to be 3.78×10^4 g/mol. The GPC result showed that the

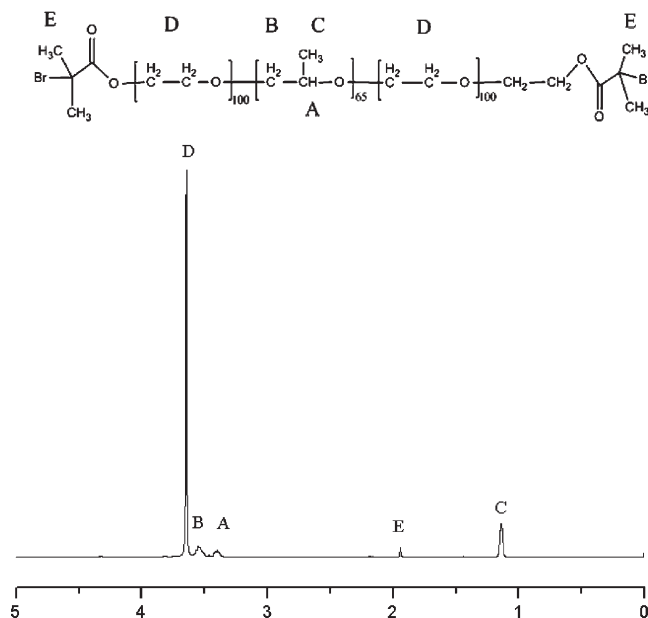


Figure 1. Structure schematic and ¹H NMR spectrum of 2-bromopropionate Pluronic F127 macroinitiator.

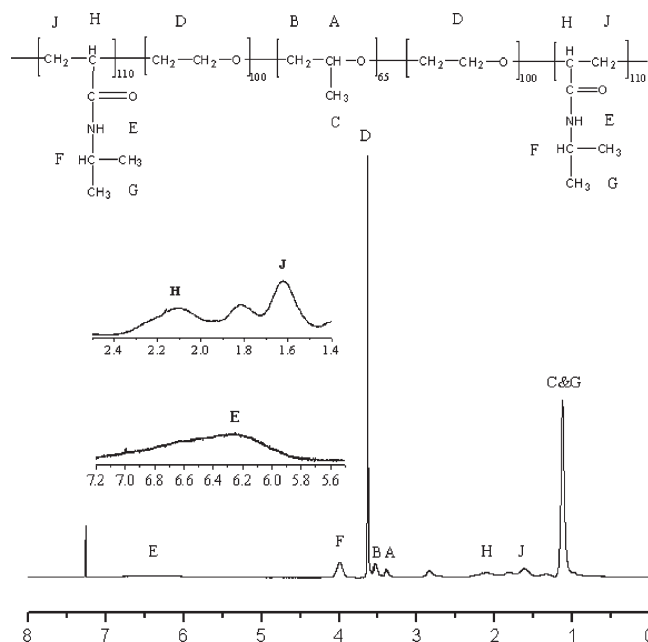


Figure 2. Structure schematic and ¹H NMR spectrum of the PNIPAm₁₁₀-F127-PNIPAm₁₁₀ pentablock terpolymer. The insets were the enlarged spectra of peaks E, H, and J.

pentablock terpolymer had narrow molecular weight distribution with $M_w/M_n = 1.14$, as shown in Figure 3. Note that the whole GPC trace was used to calculate the polydispersity, M_w/M_n . The M_n by GPC was 2.08×10^4 g/mol. Figures 2 and 3 clearly indicate that the narrow dispersed pentablock terpolymer, PNIPAm₁₁₀-F127-PNIPAm₁₁₀, was successfully obtained.

Chain Behavior of Pentablock Terpolymer in Aqueous Solution. It was well-known that Pluronic F127 and PNIPAm exhibit reversible thermosensitive characteristics in their aqueous solutions. At the low temperature, the solubility of Pluronic F127 and PNIPAm in water was attributed to the formation of hydrogen bonds between water and the polymers.^{54–58} When the temperature is raised to a given point,

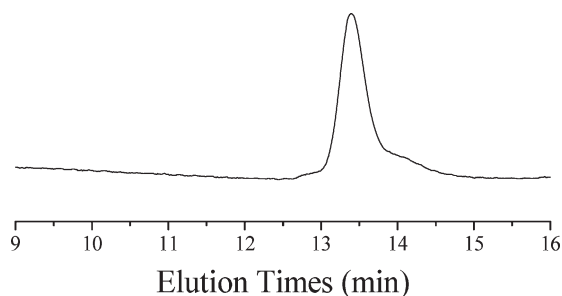


Figure 3. GPC trace of the PNIPAm₁₁₀-F127-PNIPAm₁₁₀ pentablock terpolymer.

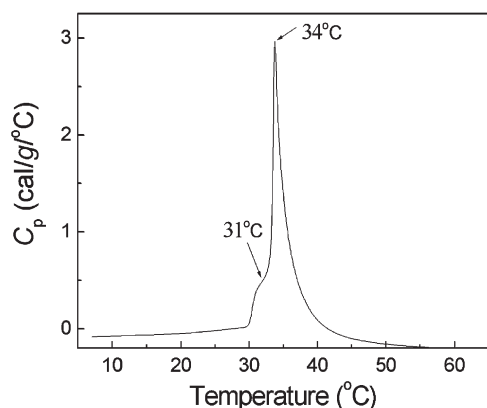


Figure 4. Temperature dependence of the specific heat capacity (C_p) for PNIPAm₁₁₀-F127-PNIPAm₁₁₀ in aqueous solution. The concentration was 0.5 mg/mL, and the heating rate was 1.0 °C/min.

known as LCST, the hydrogen bonds will be broken, which makes the PPO and PNIPAm become hydrophobic and insoluble in aqueous solution. Therefore, the PNIPAm₁₁₀-F127-PNIPAm₁₁₀ pentablock terpolymer was expected to possibly exhibit two LCSTs in its aqueous solution. The chain conformation of the PNIPAm₁₁₀-F127-PNIPAm₁₁₀ pentablock terpolymer in aqueous solution was also expected to strongly depend on the environmental temperature.

Micro-DSC was first applied to investigate the phase transition of the pentablock terpolymer in aqueous solution as a function of temperature. Figure 4 shows the micro-DSC curve of the PNIPAm₁₁₀-F127-PNIPAm₁₁₀ pentablock terpolymer in the aqueous solution with the concentrations of 0.5 mg/mL during the heating process. As expected, a bimodal transition was observed with a shoulder endothermic peak centered at 31 °C and a strong endothermic peak centered at 34 °C.

The LCST of Pluronic F127 is strongly dependent on the solution concentration and fluctuates from 10 to 80 °C as reported in the literature.^{56,58–61} The higher the concentration is, the lower the LCST is. Alexandridis et al. reported that the LCST (or the critical micellization temperature) of F127 at 0.1 wt % (corresponding to 1.0 mg/mL) was 31 °C.⁵⁶ With concentration of 2 wt % (corresponding to 20.0 mg/mL), the LCST of F127 was found to have an onset temperature of 25 °C and a peak temperature of 28 °C.⁶⁰ For the PDEAEM₂₅-*b*-F127-*b*-PDEAEM₂₅ pentablock terpolymer, the LCST of the aqueous solution of pentablock terpolymer with 2 wt % was found to be 25 °C.⁴³ Thus, on the basis of concentration used here and the literature reports, the endothermic peak at 31 °C can be attributed to the thermal phase transition of the PPO block of F127,^{54,56,60} while the endothermic peak at 34 °C can be safely attributed to the LCST of PNIPAm blocks because the LCST of PNIPAm is around 32–34 °C

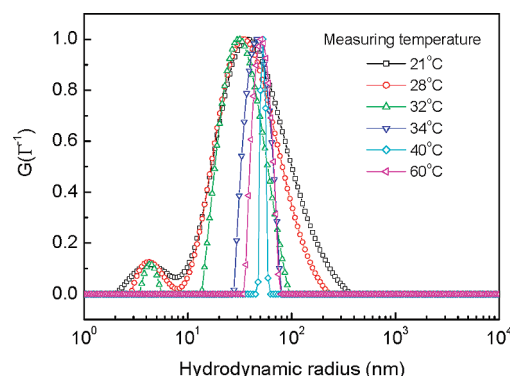


Figure 5. Distribution of hydrodynamic radius ($\langle R_h \rangle$) measured by DLS for PNIPAm₁₁₀-F127-PNIPAm₁₁₀ aqueous solution with the concentration of 0.5 mg/mL at various temperatures.

regardless of the concentrations.^{39,62–64} The micro-DSC results indicated that the PNIPAm₁₁₀-F127-PNIPAm₁₁₀ pentablock terpolymer did exhibit two LCSTs in the aqueous solution.

Static and dynamic light scattering (SLS-DLS) were then used to study the chain conformation of the PNIPAm₁₁₀-F127-PNIPAm₁₁₀ pentablock terpolymer in aqueous solution. Figure 5 shows the distribution of hydrodynamic radius ($\langle R_h \rangle$) measured by DLS for the aqueous solution of pentablock terpolymer with concentration of 0.5 mg/mL at various temperatures. Note that each measurement was carried out after the solution temperature reached its equilibrium. Interestingly, bimodal distributions were observed at the temperatures below the LCSTs of the PPO (31 °C) and PNIPAm blocks (34 °C). The center of fast relaxation mode was almost independent of temperature and corresponding to the average hydrodynamic radius ($\langle R_h \rangle$) of ca. 4.2 nm. The slow relaxation mode had wide distribution and the corresponding ($\langle R_h \rangle$) was about several tens of nanometers. Because the PEO, PPO, and PNIPAm blocks were soluble in aqueous solution at low temperature, single chain conformation may be expected for the pentablock terpolymer chains in aqueous solution at temperature < 31 °C. However, the bimodal distribution of ($\langle R_h \rangle$) strongly indicated the existence of aggregates in the aqueous solution of the pentablock terpolymer even at low temperature (for instance at 21 °C). The lengths of C–C and C–O bonds are 0.154 and 0.143 nm, respectively. If the molecular chain of PNIPAm₁₁₀-F127-PNIPAm₁₁₀ pentablock terpolymer was assumed to adopt ideal chain conformation in aqueous solution, the end-to-end distance h_0 can be roughly estimated to be $h_0 = n_1 \times l_1^2 + n_2 \times l_2^2 = 265 \times 0.451^2 + 220 \times 0.308^2 = 74.8$ nm by assuming that the lengths of monomers EO and PO were the same and the addition rule held. Note that n_1 and l_1 presented the total number and length of monomers EO and PO, respectively. n_2 and l_2 presented the total number and length of monomer NIPAm, respectively. The gyration radius, R_g , can be then estimated from the relation $\langle R_g \rangle^2 = \langle h_0 \rangle^2 / 6$ to be ca. 3.5 nm. Therefore, the fast relaxation mode can be correlated with the single chain conformation of the pentablock terpolymer in aqueous solution. The slow relaxation mode was corresponding to the aggregates formed at low temperature. For the temperature above 34 °C, only a narrow unimodal peak was observed, which had the average hydrodynamic radius ($\langle R_h \rangle$) of ca. 53 nm. It was understandable because the PPO and PNIPAm blocks were insoluble in aqueous solution at elevated temperature > 34 °C and the PNIPAm₁₁₀-F127-PNIPAm₁₁₀ pentablock terpolymer will then form micelles with hydrophobic PNIPAm and PPO blocks as cores and soluble PEO blocks as coronas.

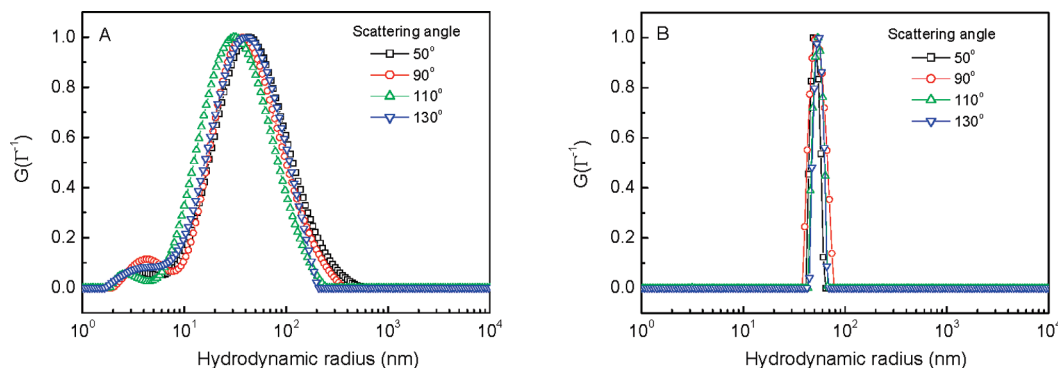


Figure 6. Distribution of hydrodynamic radius $\langle R_h \rangle$ measured by DLS for PNIPAm₁₁₀-F127-PNIPAm₁₁₀ aqueous solution with concentration of 0.5 mg/mL at various scattering angles and temperatures (A) 21 °C and (B) 38 °C.

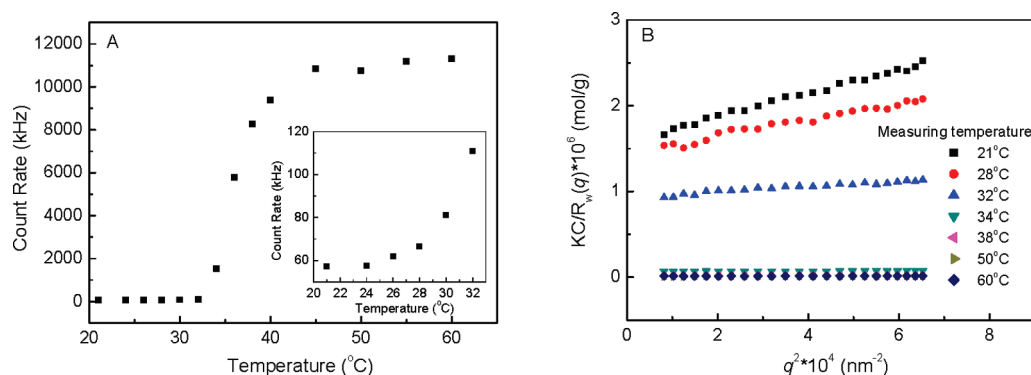


Figure 7. (A) Scattering intensities and (B) representative plots of $KC/R_{vv}(q) \sim q^2$ measured by SLS for the aqueous solution of PNIPAm₁₁₀-F127-PNIPAm₁₁₀ pentablock terpolymer with concentration of 0.5 mg/mL at various temperatures. The inset in (A) was the enlarged count rate at low temperature.

The bimodal distribution observed at low temperature for the PNIPAm₁₁₀-F127-PNIPAm₁₁₀ pentablock terpolymer in aqueous solution was not so surprising because it had been reported that PEO-containing block copolymers can form “associate” structures even the other block was soluble in water at low temperature.^{1,11–13} Topp et al. observed that the PEO-*b*-PNIPAm diblock copolymer formed aggregations in aqueous solution at the temperatures below the LCST of PNIPAm.³ Annaka and co-workers also reported that the “disordered micelles” formed by PEO-*b*-PNIPAm was started at the temperature as low as 17 °C.² Liang et al. systematically investigated the chain conformation of the PEO-containing block copolymers in aqueous solution and found that the PEO-*b*-PNIPAm diblock copolymer formed “associate” structures in the temperature well below the LCST of PNIPAm (~34 °C).¹¹ A possible mechanism of the association and aggregation was then suggested.¹¹ They also reported that the water-soluble diblock copolymer, PEO-*b*-poly(*N,N*-dimethylacrylamide) (PEO-*b*-PDMA), even formed “weak associate” structures in aqueous solution as well as in THF.¹² The DLS data shown in Figure 5 indicated that such “associate” structures were also formed in the aqueous solution of the PNIPAm₁₁₀-F127-PNIPAm₁₁₀ pentablock terpolymer at the low temperatures, for which each block was soluble. For the PNIPAm₁₁₀-F127-PNIPAm₁₁₀ pentablock terpolymer in aqueous solution, these “associate” structures might be in the kinetic equilibrium with the single chains at low temperature because the distributions of $\langle R_h \rangle$ measured by DLS at 21 °C were fluctuated and dependent on the scattering angles, as shown in Figure 6A. Furthermore, the micelles formed at high temperature (38 °C) were uniformly distributed and almost independent of the scattering angles (Figure 6B).

Figure 7 shows the scattering intensities (namely count rate) and the representative plots of $KC/R_{vv}(q) \sim q^2$ measured by SLS at various temperatures for the same aqueous solution of the PNIPAm₁₁₀-F127-PNIPAm₁₁₀ pentablock terpolymer (0.5 mg/mL). Note that the scattering intensities had been normalized to the same incident intensity. The scattering intensity (count rate) of the solution was fairly weak and ca. 50 kHz at 21 °C (Figure 7A), which may indicate that dilute particles or particles with very loose structure exist in the solution. The count rate slowly increased with increasing the temperature from 21 to 32 °C as shown in the inset of Figure 7A. However, when the temperature was increased above 34 °C, the count rate increased sharply and reached as high as 10910 kHz at 60 °C, which strongly indicated the formation of big aggregates above 34 °C. Figure 7B shows that the excess scattering intensity $R_{vv}(q)$ exhibited strongly angular dependence at the low temperature. The apparent weight-average molecular weight ($M_{w,app}$) and the Z-average root-mean-square radius (R_g) of the pentablock terpolymer chains or “associates” or micelles were then calculated by fitting the plots of $KC/R_{vv}(q) \sim q^2$ with eq 1. The so-called aggregation number N can be also estimated from the calculated $M_{w,app}$ and M_n of the pentablock terpolymer measured by ¹H NMR. Figure 8 shows the temperature dependence of the obtained $M_{w,app}$ and the corresponding N for the aqueous solution of the PNIPAm₁₁₀-F127-PNIPAm₁₁₀ pentablock terpolymer with concentration of 0.5 mg/mL. Note that the experimental data from the three other samples with different concentrations are also included in Figure 8. The $M_{w,app}$ and N clearly indicated that the molecular chains of the pentablock terpolymer in aqueous solution formed “associate” at 21 °C although the PEO, PPO, and PNIPAm blocks were dissolved in water at this

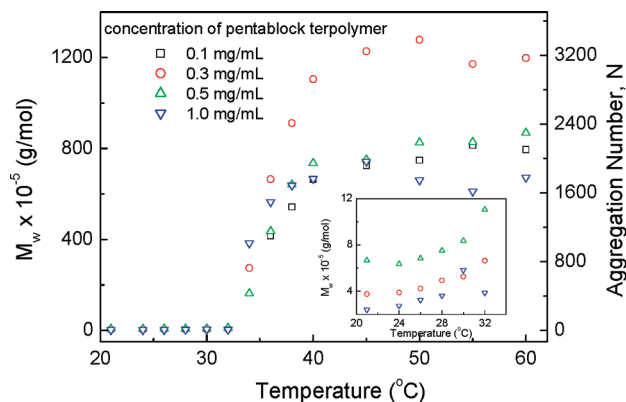


Figure 8. Apparent weight-average molecular weight $M_{w,app}$ and the corresponding aggregation number N of the PNIPAm₁₁₀-F127-PNIPAm₁₁₀ pentablock terpolymer chains, “associate”, and micelles in the aqueous solutions as the function of temperature. Four samples with various concentrations were measured.

temperature. Similarly, $M_{w,app}$ and N slowly increased with increasing the temperature from 21 to 32 °C and increased strongly when the temperature was above 34 °C. The plateau values of $M_{w,app}$ and N were observed in the temperature range of 38–60 °C, indicating the formation of stable micelles. These results were different from the observation of PEO-*b*-PNIPAm diblock copolymer in aqueous solution by Yan et al.,¹¹ who observed a continuous increase of $M_{w,app}$ from 25 to 55 °C. However, for the PNIPAm-*g*-PEO in aqueous solution, Qin et al. found that stable mesoglobules were formed at temperature above ~42 °C, where the inter-chain association stopped.⁶⁵

Figure 9 shows the hydrodynamic radius, $\langle R_h \rangle$, obtained by DLS and the gyration radius, $\langle R_g \rangle$, by SLS of the PNIPAm₁₁₀-F127-PNIPAm₁₁₀ pentablock terpolymer in the aqueous solution with concentration of 0.5 mg/mL as a function of temperature. Note that for the temperature below 34 °C the hydrodynamic radius, $\langle R_h \rangle$, was calculated from the slow relaxation mode and presented the size of “associate” in the aqueous solution. It can be seen that the evolution of $\langle R_h \rangle$ as the function of temperature can be divided into four regions: (I) $\langle R_h \rangle$ was around 36 nm in the temperature range of 21–28 °C; (II) $\langle R_h \rangle$ showed a decrease from 37 nm at 28 °C to 31.5 nm at 32 °C; (III) $\langle R_h \rangle$ strongly increased from 31.5 to 53 nm when the temperature was increased from 32 to 38 °C; (IV) $\langle R_h \rangle$ reached a plateau value of ca. 53 nm for the temperature range of 38–60 °C. The gyration radius $\langle R_g \rangle$ decreased with increasing the temperature and also reached a plateau value of ca. 32 nm for the temperature range of 34–60 °C. A strong decrease of $\langle R_g \rangle$ from ca. 50 to 32 nm was also observed when the temperature was increased from 28 to 32 °C. $\langle R_h \rangle$ was smaller than $\langle R_g \rangle$ at temperature < 34 °C, while $\langle R_h \rangle$ was much larger than $\langle R_g \rangle$ at temperature > 34 °C.

The cloud point of the aqueous solution of PNIPAm₁₁₀-F127-PNIPAm₁₁₀ pentablock terpolymer was consistent with the results of light scattering measurements. Figure 10 shows the optical transmittance at 400 nm as the function of measuring temperature for the aqueous solutions of the pentablock terpolymer with concentrations of 0.3 and 0.5 mg/mL. For both solutions, the transmittance started to strongly decrease at 34 °C and leveled off above 50 °C. The cloud point of the pentablock terpolymer in aqueous solution was then determined to be 34 °C, which was consistent with the temperature at which the hydrodynamic radius increased dramatically (cf. Figure 9). At 60 °C, the aqueous

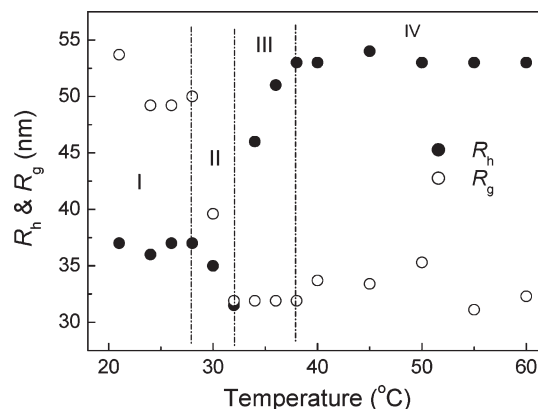


Figure 9. $\langle R_h \rangle$ and $\langle R_g \rangle$ of the PNIPAm₁₁₀-F127-PNIPAm₁₁₀ pentablock terpolymer chains, “associate”, and micelles in the aqueous solution with concentration of 0.5 mg/mL as a function of temperature.

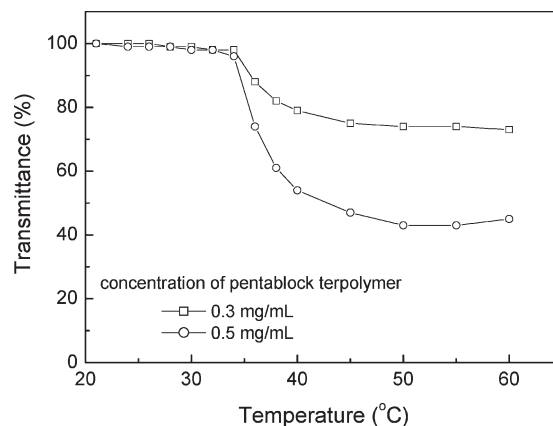


Figure 10. Optical transmittance at 400 nm as a function of measuring temperature for the aqueous solutions of the pentablock terpolymer with concentrations of 0.3 and 0.5 mg/mL.

solutions of the pentablock terpolymer appeared blue tint, indicating the formation of micelles.

To get insight into the microstructures of the pentablock terpolymer chains in aqueous solution, the ratio of $\langle R_g \rangle / \langle R_h \rangle$ was calculated and plotted as a function of temperature in Figure 11. Note that the $\langle R_g \rangle / \langle R_h \rangle$ data from the three other samples with different concentrations are also included in Figure 11. The value of $\langle R_g \rangle / \langle R_h \rangle$ reflects the conformation and architecture of a polymer chain in solution or the cross-linking density distribution of the microgels.^{66–68} For example, for linear and flexible polymer chains, $\langle R_g \rangle / \langle R_h \rangle$ is around 1.5, while for uniform hard spheres, $\langle R_g \rangle / \langle R_h \rangle$ is 0.778. For the temperatures below 28 °C, where water is a fairly good solvent for PEO, PPO, and PNIPAm, $\langle R_g \rangle / \langle R_h \rangle$ was ~1.32–1.45, close to 1.5 for linear flexible coil chains. However, the values of $\langle R_g \rangle$ and $\langle R_h \rangle$ were much larger than the size of single coil chain of the PNIPAm₁₁₀-F127-PNIPAm₁₁₀ pentablock terpolymer in good solvent. The $\langle R_g \rangle$ and $\langle R_h \rangle$ together with the ratio of $\langle R_g \rangle / \langle R_h \rangle$ suggested that the pentablock terpolymer chains formed loose “associate” at the low temperature, which was similar to those observed in several PEO-containing block copolymer systems.^{1,11–13} $\langle R_g \rangle / \langle R_h \rangle$ decreased from 1.35 to 1.0 when increasing the temperature from 28 to 32 °C. Together with the data shown in Figure 9, the decrease of $\langle R_g \rangle / \langle R_h \rangle$ can be attributed to the dehydration of PPO block in the temperature range of 28–32 °C. It has been reported that the dehydration process of PPO began at a temperature lower than that of the LCST of

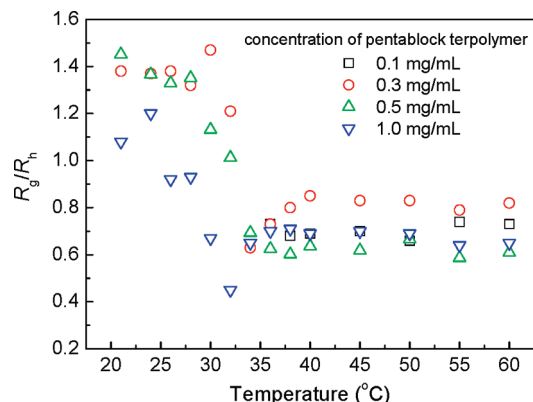


Figure 11. R_g/R_h ratios of the PNIPAm₁₁₀-F127-PNIPAm₁₁₀ pentablock terpolymer chains, “associate”, and micelles in the aqueous solution as a function of temperature. Four samples with various concentrations were measured.

F127.⁵⁶ The micro-DSC result (Figure 4) showed that the LCST of PPO was ca. 31 °C. Therefore, it was reasonable to believe that the PPO chains started to collapse and shrink in the core of the association at 28 °C, leading to the decrease of $\langle R_g \rangle$ and $\langle R_h \rangle$ from 28 to 32 °C. Furthermore, the continuous increase of $M_{w,app}$ from 28 to 32 °C (cf. Figure 8) may suggest that the interchain association and intrachain contraction proceeded at the same time in this region. When the temperature was above 34 °C, $\langle R_g \rangle/\langle R_h \rangle$ reached a nearly constant value of ca. 0.62, which indicated the formation of core-shell micelles with dense cores and loose shells.⁶⁵ The LCST of PNIPAm blocks was ca. 34 °C and higher than that of PPO block as measured by micro-DSC. As expected, when the temperature was higher than 34 °C, the PPO and PNIPAm blocks were hydrophobic and formed the cores and the PEO blocks were hydrophilic and formed the coronas of the micelles. The collapsed PPO and PNIPAm core had a higher chain density than that of swollen PEO coronas, leading to the smaller $\langle R_g \rangle/\langle R_h \rangle$ than that of the uniform sphere. The strong increase of $\langle R_h \rangle$ from 31.5 nm at 32 °C to 53 nm at 38 °C indicated the collapse of PPO and PNIPAm chains and the formation of micelles. The transformation from loose “associate” to micelles was not only due to the collapse of PPO and PNIPAm chains into the core of the “associate” but more importantly due to the rearrangement of the shrinking “associate” and collapsed PPO and PNIPAm chains. If there was not significant rearrangement, both $\langle R_h \rangle$ and $\langle R_g \rangle$ should continuously decrease with increasing temperature as those observed for the PEO-*b*-PNIPAm diblock copolymer in aqueous solution.¹¹ Yan et al. observed a sharp reduction in size of PEO-*b*-PNIPAm aggregates when the temperature was well above the cloud point of PNIPAm from 42 to 55 °C.¹¹ However, a strong increase of $\langle R_h \rangle$ was observed for the pentablock terpolymer in aqueous solution when the temperature was above the LCST of PPO and PNIPAm blocks from 32 to 38 °C and a plateau value of $\langle R_h \rangle$ at temperature > 38 °C was reached. Therefore, it was speculated that the shrinking “associate” was rearranged into the core-shell micelles with dense collapsed PPO and PNIPAm cores and loose swollen PEO coronas during the collapsing process of PNIPAm and PPO chains in the temperature range of 32–38 °C. The interchain association and intrachain contraction almost stopped in the region IV (> 38 °C) as evidenced by the almost constant values of $M_{w,app}$, $\langle R_h \rangle$, and $\langle R_g \rangle$, indicating the formation of stable micelles with dense PPO and PNIPAm cores and swollen PEO coronas.

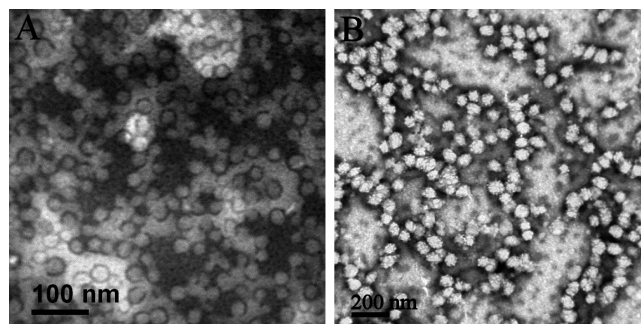


Figure 12. TEM images of the PNIPAm₁₁₀-F127-PNIPAm₁₁₀ pentablock terpolymer in aqueous solution with concentration of 0.5 mg/mL. (A) The “associates” formed at 21 °C and (B) the micelles formed at 38 °C.

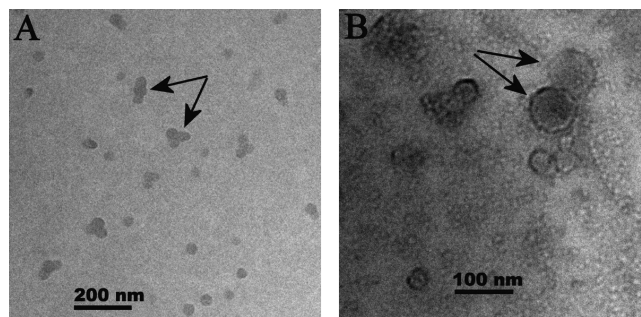


Figure 13. Cryo-TEM images of the PNIPAm₁₁₀-F127-PNIPAm₁₁₀ pentablock terpolymer in aqueous solution with concentration of 0.5 mg/mL. (A) The “associates” formed at 21 °C and (B) the micelles formed at 38 °C.

Visible images of the “associate” and micelles of the PNIPAm₁₁₀-F127-PNIPAm₁₁₀ pentablock terpolymer in aqueous solution were also obtained by TEM investigation. Figure 12 shows the TEM morphologies of the “associate” and the micelles of the PNIPAm₁₁₀-F127-PNIPAm₁₁₀ pentablock terpolymer in aqueous solution with a concentration of 0.5 mg/mL at 21 and 38 °C, respectively. Many spherical-like particles together with dried patches of the pentablock terpolymer chains were observed at 21 °C (Figure 12A). These spherical particles were attributed to the “associates” formed at 21 °C. The size of the particles was ca. 32 ± 2 nm, which was much smaller than the hydrodynamic diameter of the “associate” (ca. 72 nm) measured by DLS. It was reasonable because the “associate” had loose structures and contained large amounts of water inside. The drying process during the sample preparation on the Formvar-coated copper grids made the “associate” shrink, leading to the smaller size observed by TEM. At 38 °C, spherical micelles with rather uniform size of ca. 87 ± 8 nm were observed (Figure 12B), which was much larger than that of ca. 32 nm for the “associate” formed at 21 °C and close to that of ca. 106 nm by DLS. It was acceptable because the micelles formed at higher temperature had more dense structures although the size of dried micelles was still smaller than the size of swollen micelles in solution. Figure 13 shows the corresponding cryo-TEM images. The arrows in Figure 13A clearly indicated the “associates” of the PNIPAm₁₁₀-F127-PNIPAm₁₁₀ pentablock terpolymer formed in aqueous solution at 21 °C. At 38 °C, the PNIPAm₁₁₀-F127-PNIPAm₁₁₀ pentablock terpolymer formed micelles in aqueous solution, of which the sizes were close to the results by DLS, as shown in Figure 13B. The TEM and cryo-TEM results were consistent with the DLS and SLS data, confirming the coexistence of the “associates”

Table 1. $\langle R_h \rangle$, $\langle R_g \rangle$, and $\langle R_g \rangle / \langle R_h \rangle$ of the PNIPAm₁₁₀-F127-PNIPAm₁₁₀ Pentablock Terpolymer in the Aqueous Solutions with Various Concentrations as a Function of Temperature

temp (°C)	0.1 mg/mL			0.3 mg/mL			0.5 mg/mL			1.0 mg/mL		
	R_g (nm)	R_h (nm)	R_g/R_h	R_g (nm)	R_h (nm)	R_g/R_h	R_g (nm)	R_h (nm)	R_g/R_h	R_g (nm)	R_h (nm)	R_g/R_h
21				51	37	1.38	54	37	1.45	28	26	1.08
24				52	38	1.37	49	36	1.36	30	25	1.20
26				51	37	1.37	49	37	1.33	24	26	0.92
28				49	37	1.32	50	37	1.35	25	27	0.93
30				47	32	1.47	39	35	1.13	18	27	0.67
32				41	34	1.21	32	32	1.01	18	40	0.45
34				34	54	0.63	32	46	0.69	41	63	0.65
36	37	51	0.73	44	60	0.73	32	51	0.62	46	66	0.70
38	36	53	0.68	49	61	0.80	32	53	0.60	47	66	0.71
40	37	54	0.69	52	61	0.85	33	53	0.64	46	67	0.69
45	37	53	0.70	53	64	0.83	33	54	0.62	46	66	0.70
50	35	53	0.66	52	63	0.83	35	53	0.67	45	65	0.69
55	39	53	0.74	50	63	0.79	31	53	0.59	41	64	0.64
60	38	52	0.73	50	61	0.82	32	53	0.61	41	63	0.65

and single chains for the PNIPAm₁₁₀-F127-PNIPAm₁₁₀ pentablock terpolymer in aqueous solution at low temperature and the formation of big dense micelles at higher temperature above the LCST of PNIPAm blocks.

The effects of the concentration on the chain behavior of the PNIPAm₁₁₀-F127-PNIPAm₁₁₀ pentablock terpolymer in aqueous solution were also investigated. Aqueous solutions of the pentablock terpolymer with concentrations of 0.1, 0.3, and 1.0 mg/mL were also studied. Similar phenomena were observed. The existence of “associate” at low temperature and the formation of big dense micelles were observed for all the aqueous solutions of the pentablock terpolymer regardless of the concentration. The values of $\langle R_h \rangle$, $\langle R_g \rangle$, and $\langle R_g \rangle / \langle R_h \rangle$ are summarized in Table 1. The ratio of $\langle R_g \rangle / \langle R_h \rangle$ is also plotted in Figure 11. It should be noted that the sample with 0.1 mg/mL was too dilute so that the scattering intensity at temperature below 34 °C was very weak, and $\langle R_g \rangle$ and $\langle R_h \rangle$ cannot be accurately measured by SLS and DLS. The apparent weight-average molecular weight $M_{w,app}$ and the corresponding aggregation number N are included in Figure 8. It can be seen that at the temperature below 34 °C $\langle R_g \rangle$ and $\langle R_h \rangle$ were smaller for the aqueous solution of pentablock terpolymer with higher concentration than those with lower concentration. These results were consistent with the findings of Yan et al., who found that the increase of concentration will against the formation of “associate” at low temperature for PEO-*b*-PNIPAm diblock copolymer in aqueous solutions.¹¹ However, at temperature above 34 °C, the solution concentration had less effect on $\langle R_h \rangle$, $\langle R_g \rangle$, and $\langle R_g \rangle / \langle R_h \rangle$ of the micelles of pentablock terpolymer. No obvious tendency can be obtained. Again, the stable core-shell micelles were formed at temperature > 38 °C for all the three aqueous solutions of the PNIPAm₁₁₀-F127-PNIPAm₁₁₀ pentablock terpolymer, as evidenced by the almost constant values of $M_{w,app}$, $\langle R_h \rangle$, $\langle R_g \rangle$, and $\langle R_g \rangle / \langle R_h \rangle$ (cf. Figures 8 and 11, Table 1).

Conclusions

The narrow dispersed PNIPAm₁₁₀-F127-PNIPAm₁₁₀ pentablock terpolymer was successfully synthesized by the typical ATRP method using NIPAm as the monomer and modified F127 as the macroinitiator. The pentablock terpolymer showed double thermosensitive behavior and exhibited two LCSTs at 31 and 34 °C in the aqueous solution, which can be attributed to the thermal phase transition of the PPO block and the PNIPAm blocks, respectively. The SLS-DLS results indicated that loose “associates” and single coil chains coexisted in the aqueous solution of the pentablock terpolymer chains at the low temperature (21–28 °C), where the PEO, PPO, and PNIPAm blocks were

soluble in water. A transition region from 28 to 32 °C was observed, where the interchain association and intrachain contraction occurred simultaneously, leading to the decrease of $\langle R_h \rangle$ and $\langle R_g \rangle$ and the increase of $M_{w,app}$. In the temperature range of 32–38 °C, the interchain association and rearrangement of the shrinking “associates” dominated, which was evidenced by the strong increase of $\langle R_h \rangle$ and $M_{w,app}$. At the high temperature (38–60 °C), the interchain association and intrachain contraction almost stopped, and the pentablock terpolymer chains formed large and stable core-shell micelles with collapsed PPO and PNIPAm cores and swollen PEO shells. The TEM and cryo-TEM images were consistent with the SLS-DLS results, confirming the formation of loose “associates” at 21 °C and large stable micelles at 38 °C. At low temperature, increase of concentration will hinder the formation of “associate”. However, the micelles formed at high temperature were found to be almost independent of the solution concentration investigated in the present work.

Acknowledgment. We thank the National Natural Science Foundation of China (20604022, 20874087) and 863 project (No. 2009AA04Z125) for financial support. We thank Prof. Guangzhao Zhang and Dr. Weizhong Chen at the University of Science and Technology of China for the help in the DLS-SLS measurements and fruitful discussions. We thank Ms. Yinyin Li at Sun Yat-Sen University for her help in the cryo-TEM measurements.

References and Notes

- Huang, X. N.; Du, F. S.; Cheng, J.; Dong, Y. Q.; Liang, D. H.; Ji, S. P.; Lin, S. S.; Li, Z. C. *Macromolecules* **2009**, *42*, 783.
- Motokawa, R.; Morishita, K.; Koizumi, S.; Nakahira, T.; Annaka, M. *Macromolecules* **2005**, *38*, 5748.
- Topp, M. D. C.; Dijkstra, P. J.; Talsma, H.; Feijen, J. *Macromolecules* **1997**, *30*, 8518.
- Riess, G. *Prog. Polym. Sci.* **2003**, *28*, 1107.
- Burke, S.; Shen, H. W.; Eisenberg, A. *Macromol. Symp.* **2001**, *175*, 273.
- Luo, L. B.; Eisenberg, A. *J. Am. Chem. Soc.* **2001**, *123*, 1012.
- Zhang, L. F.; Eisenberg, A. *Polym. Adv. Technol.* **1998**, *9*, 677.
- Zhulina, E. B.; Adam, M.; LaRue, I.; Sheiko, S. S.; Rubinstein, M. *Macromolecules* **2005**, *38*, 5330.
- Zhu, J. T.; Yu, H. Z.; Jiang, W. *Eur. Polym. J.* **2008**, *44*, 2275.
- Li, X. J.; Deng, M. G.; Liu, Y.; Liang, H. J. *J. Phys. Chem. B* **2008**, *112*, 14762.
- Yan, J. J.; Ji, W. X.; Chen, E. Q.; Li, Z. C.; Liang, D. H. *Macromolecules* **2008**, *41*, 4908.
- Ke, F. Y.; Mo, X. L.; Yang, R. M.; Wang, Y. M.; Liang, D. H. *Macromolecules* **2009**, *42*, 5339.
- Kriz, J.; Dybal, J. *J. Phys. Chem. B* **2010**, *114*, 3140.
- Du, B. Y.; Mei, A. X.; Yin, K. Z.; Zhang, Q. F.; Xu, J. T.; Fan, Z. Q. *Macromolecules* **2009**, *42*, 8477.
- Antonietti, M.; Forster, S. *Adv. Mater.* **2003**, *15*, 1323.
- Discher, B. M.; Won, Y. Y.; Ege, D. S.; Lee, J. C. M.; Bates, F. S.; Discher, D. E.; Hammer, D. A. *Science* **1999**, *284*, 1143.

- (17) Discher, D. E.; Eisenberg, A. *Science* **2002**, 297, 967.
- (18) Zhang, Q.; Ye, J.; Lu, Y.; Nie, T.; Xie, D.; Song, Q.; Chen, H.; Zhang, G.; Tang, Y.; Wu, C.; Xie, Z. *Macromolecules* **2008**, 41, 2228.
- (19) Hong, L. Z.; Zhu, F. M.; Li, J. F.; Ngai, T.; Xie, Z. W.; Wu, C. *Macromolecules* **2008**, 41, 2219.
- (20) Determan, M. D.; Guo, L.; Thiagarajan, P.; Mallapragada, S. K. *Langmuir* **2006**, 22, 1469.
- (21) Zhou, Y. M.; Jiang, K. Q.; Song, Q. L.; Liu, S. Y. *Langmuir* **2007**, 23, 13076.
- (22) Lintuvuori, J. S.; Wilson, M. R. *Phys. Chem. Chem. Phys.* **2009**, 11, 2116.
- (23) Gindy, M. E.; Prud'homme, R. K.; Panagiotopoulos, A. Z. *J. Chem. Phys.* **2008**, 128, 164906.
- (24) Hugouvieux, V.; Axelos, M. A. V.; Kolb, M. *Macromolecules* **2009**, 42, 392.
- (25) Reinhout, I. C.; Cornelissen, J.; Nolte, R. J. M. *J. Am. Chem. Soc.* **2007**, 129, 2327.
- (26) LaRue, I.; Adam, M.; Pitsikalis, M.; Hadjichristidis, N.; Rubinstein, M.; Sheiko, S. S. *Macromolecules* **2006**, 39, 309.
- (27) Du, H. B.; Zhu, J. T.; Jiang, W. J. *Phys. Chem. B* **2007**, 111, 1938.
- (28) Choucair, A.; Eisenberg, A. *Eur. Phys. J. E* **2003**, 10, 37.
- (29) Yu, G. E.; Eisenberg, A. *Macromolecules* **1998**, 31, 5546.
- (30) Burke, S. E.; Eisenberg, A. *Langmuir* **2001**, 17, 6705.
- (31) Chen, Z. Y.; Cui, H. G.; Hales, K.; Li, Z. B.; Qi, K.; Pochan, D. J.; Wooley, K. L. *J. Am. Chem. Soc.* **2005**, 127, 8592.
- (32) Hadjiantoniou, N. A.; Trifitaridou, A. I.; Kafouris, D.; Gradzielski, M.; Patrickios, C. S. *Macromolecules* **2009**, 42, 5492.
- (33) Sommerdijk, N.; Holder, S. J.; Hiorns, R. C.; Jones, R. G.; Nolte, R. J. M. *Macromolecules* **2000**, 33, 8289.
- (34) Hong, J.; Wang, Q.; Lin, Y. Z.; Fan, Z. Q. *Macromolecules* **2005**, 38, 2691.
- (35) Lei, P.; Wang, Q.; Hong, J.; Li, Y. X. *J. Polym. Sci., Polym. Chem.* **2006**, 44, 6600.
- (36) Zhang, L. S.; Wang, Q.; Lei, P.; Wang, X.; Wang, C. Y.; Cai, L. *J. Polym. Sci., Polym. Chem.* **2007**, 45, 2617.
- (37) Hong, J.; Wang, Q.; Fan, Z. Q. *Macromol. Rapid Commun.* **2006**, 27, 57.
- (38) Du, B. Y.; Mei, A. X.; Yang, Y.; Zhang, Q. F.; Wang, Q.; Xu, J. T.; Fan, Z. Q. *Polymer* **2010**, 51, 3493.
- (39) Zhang, G. Z.; Winnik, F. M.; Wu, C. *Phys. Rev. Lett.* **2003**, 90, 035506.
- (40) Kriksin, Y. A.; Khalatur, P. G.; Khokhlov, A. R. *J. Chem. Phys.* **2005**, 122, 114703.
- (41) Bhattacharya, S.; Hsu, H. P.; Milchev, A.; Rostsiashvili, V. G.; Vilgis, T. A. *Macromolecules* **2008**, 41, 2920.
- (42) Sumithra, K.; Brandau, M.; Straube, E. *J. Chem. Phys.* **2009**, 130, 234901.
- (43) Determan, M. D.; Cox, J. P.; Seifert, S.; Thiagarajan, P.; Mallapragada, S. K. *Polymer* **2005**, 46, 6933.
- (44) Peleshanko, S.; Anderson, K. D.; Goodman, M.; Determan, M. D.; Mallapragada, S. K.; Tsukruk, V. V. *Langmuir* **2007**, 23, 25.
- (45) Storey, R. F.; Scheuer, A. D.; Achord, B. C. *Polymer* **2005**, 46, 2141.
- (46) Harada, T.; Bates, F. S.; Lodge, T. P. *Macromolecules* **2003**, 36, 5440.
- (47) Sha, K.; Li, D. S.; Li, Y. P.; Zhang, B.; Wang, J. Y. *Macromolecules* **2008**, 41, 361.
- (48) Hadjiantoniou, N. A.; Krasia-Christoforou, T.; Loizou, E.; Porcar, L.; Patrickios, C. S. *Macromolecules* **2010**, 43, 2713.
- (49) Tsitsilianis, C.; Stavrouli, N.; Bocharova, V.; Angeiopoulos, S.; Kiri, A.; Katsampas, I.; Stamm, M. *Polymer* **2008**, 49, 2996.
- (50) Zhang, L. F.; Cheng, Z. P.; Zhou, N. C.; Zhang, R. M.; Zhu, X. L. *Macromol. Symp.* **2008**, 261, 54.
- (51) He, J. L.; Ni, P. H.; Liu, C. C. *J. Polym. Sci., Polym. Chem.* **2008**, 46, 3029.
- (52) Wu, L. F.; Cochran, E. W.; Lodge, T. P.; Bates, F. S. *Macromolecules* **2004**, 37, 3360.
- (53) Wu, C.; Xia, K. Q. *Rev. Sci. Instrum.* **1994**, 65, 587.
- (54) Wanka, G.; Hoffmann, H.; Ulbricht, W. *Macromolecules* **1994**, 27, 4145.
- (55) Schild, H. G. *Prog. Polym. Sci.* **1992**, 17, 163.
- (56) Alexandridis, P.; Holzwarth, J. F.; Hatton, T. A. *Macromolecules* **1994**, 27, 2414.
- (57) Kjellander, R.; Florin, E. *J. Chem. Soc., Faraday Trans.* **1981**, 77, 2053.
- (58) Guo, C.; Wang, J.; Liu, H. Z.; Chen, J. Y. *Langmuir* **1999**, 15, 2703.
- (59) Zhao, F.; Xie, D. H.; Zhang, G. Z.; Pispas, S. *J. Phys. Chem. B* **2008**, 112, 6358.
- (60) Lam, Y. M.; Grigorieff, N.; Goldbeck-Wood, G. *Phys. Chem. Chem. Phys.* **1999**, 1, 3331.
- (61) Ye, X. D.; Lu, Y. J.; Liu, S. L.; Zhang, G. Z.; Wu, C. *Langmuir* **2007**, 23, 10366.
- (62) Qiu, X. P.; Kwan, C. M. S.; Wu, C. *Macromolecules* **1997**, 30, 6090.
- (63) Qiu, X. P.; Wu, C. *Macromolecules* **1997**, 30, 7921.
- (64) Gao, J.; Wu, C. *Macromolecules* **1997**, 30, 6873.
- (65) Chen, H. W.; Zhang, Q. J.; Li, J. F.; Ding, Y. W.; Zhang, G. Z.; Wu, C. *Macromolecules* **2005**, 38, 8045.
- (66) Senff, H.; Richtering, W. *J. Chem. Phys.* **1999**, 111, 1705.
- (67) Kuckling, D.; Vo, C. D.; Adler, H. J. P.; Volkel, A.; Colfen, H. *Macromolecules* **2006**, 39, 1585.
- (68) Chen, H. W.; Li, J. F.; Ding, Y. W.; Zhang, G. Z.; Zhang, Q. J.; Wu, C. *Macromolecules* **2005**, 38, 4403.